Garcia-Reinoso; J., Hernández, J. A., Seoane, I. & Vidal, I. (2014). On the effect of sudden data bursts in the upstream channel of Ethernet PONs employing IPACT under the gated-service discipline. *Optical Switching and Networking* 13, pp. 94-102.

DOI: 10.1016/j.osn.2014.02.004

On the effect of sudden data bursts in the upstream channel of Ethernet PONs employing IPACT under the gated-service discipline

J. Garcia-Reinoso*, J.A. Hernández, I. Seoane, I. Vidal

Avda. de la Universidad 30, 28911 Leganés, Madrid, Spain

A B S T R A C T

The Interleaved Polling with Adapted Cycle Times (IPACT) algorithm for dynamic bandwidth allocation proposed for Ethernet Passive Optical Networks (EPONs) has been deeply analysed in the literature under Poisson traffic. However, the case when ONUs suddenly offer bursty traffic in the upstream channel of a PON has not been considered in such detail.

This paper studies the performance behaviour of the upstream channel of EPONs employing IPACT with the gated-service disciple, under Poisson traffic together with sudden bursts. We show that one burst arrival produces a peak in the average transmission window of every ONU, lasting its effects for several cycle times, depending on the burst size and the average network load. Such a burst has a direct impact on the delay experienced by the packets of other ONUs. This is mathematically modelled using a modification of the formerly studied M/G/1 queue with vacations and validated with simulation.

Keywords: Passive Optical Networks - Interleaved Polling with Adapted Cycle Times -Gated service -Teletraffic analysis -Average queueing delay

1. Introduction

Passive Optical Networks (PONs) have been proposed in the literature to open up the access bottleneck of residential users [1]. The Ethernet PON (EPON) and Gigabit PON (GPON) standards, under deployment by many operators, allow 1 Gbit/s of upstream bandwidth shared between 32 and 64 (even 128) end users via TDM. In EPON, the Interleaved Polling with Adaptive Cycle Times (IPACT) has been proposed as a Dynamic Bandwidth Algorithm (DBA) to arbitrate channel access while reducing bandwidth waste. In IPACT, the Optical Network Units (ONUs) request transmission windows for their accumulated traffic to the Optical Line Terminal (OLT), which may grant all or part of it [2,3]. The OLT arbitrates channel access, and decides which ONU transmits, when and for how long.

The average cycle time in IPACT, that is, the amount of time elapsed between two consecutive transmission windows for the same ONU, has been demonstrated to depend on the number of ONUs, guard time and total upstream load for Poisson traffic [4,5]. Several studies have focused on studying the properties of the upstream TDM-shared channel of a PON under Poisson traffic. For instance, the authors in [6] studied the average delay experienced by a packet selected at random in the upstream channel of a PON. Essentially, the analysis carried out comprises a modification of the formerly studied M/G/1 queue with vacations derived in [7].

The number of research studies focused on the upstream channel of TDM PONs has increased in the previous years, covering many interesting aspects. For instance, the authors

* Corresponding author.
E-mail addresses: jgr@it.uc3m.es (J. Garcia-Reinoso), jahgutie@it.uc3m.es (J.A. Hernández), iseoane@it.uc3m.es (I. Seoane), ividal@it.uc3m.es (I. Vidal).

in [8] show that the position of the Report message within the time window has a direct impact on the delay experienced by the packets in the upstream channel; and they further propose an adaptive mechanism to find the optimal position of this message at a given network load.

While IPACT is very efficient in terms of uplink bandwidth utilisation, it does not address QoS (Quality of Service) guarantees for the individual ONUs in the network. In light of this, the authors in [9] propose a new DBA algorithm (under the name of Distributed Dynamic Scheduling, also known as DDSPON) to dynamically allocate bandwidth with guaranteed QoS to ONUs. In [10], the authors study the delay variation of frames in the upstream of a PON and further propose an algorithm to never breach a certain threshold. In [11], the authors propose a mechanism to drop low-priority packets under high-loads to benefit high-priority packets with tight delay constraints.

Analysis extensions for the Next-Generation Passive Optical Networks (NG-PON) with high capacity and long-reach, but still TDM-based, have also been proposed in the literature [12,13]. The case of hybrid TDM/WDM PONs has been covered in [14].

Finally, other studies have focused on using some of the previous models to study the on/off cycles of ONUs in a PON on attempts to estimate whether or not part of the ONUs' hardware can be switched off to save energy. Examples of these studies are: [15–18].

However, most of these studies assume that the ONUs offer Poisson traffic in the upstream channel. To the best of the authors' knowledge, none of the above papers have addressed the impact of bursty traffic arrivals at the ONUs. Such bursty traffic typically appears (but it is not restricted to) in video-streaming scenarios, whereby video-streaming servers continuously produce I, P or B frames of several tens of kilobytes [19,20]. Such an interesting traffic pattern (bursts of 20–80 1500-byte packets) has not yet been analysed mathematically. Essentially, the ONU with the periodic bursty traffic is expected to seldomly request very large transmission windows, thus introducing very long delays to other ONUs, when gated-service discipline is used. This paper aims at analysing the impact of traffic bursts in the average cycle time and average delay experienced by individual packets during the burst transmission and in subsequent cycles.

The remainder of this paper is organised as follows: Section 2 reviews the state of the art in the modelling of IPACT and the delay experienced by packets in the upstream channel under Poisson traffic. Section 3 extends this methodology to deal with data burst arrivals and transmissions. Section 4 validates the results and equations obtained with simulation. Finally, Section 5 concludes this work with a summary of its main contributions and discussion.

2. Analysis of average cycle times with gated-service

2.1. Problem statement: gated service review

Consider the PON of Fig. 1(a). Fig. 1(b) shows an example of two cycle times as observed by the third ONU in the PON. Here, $V_i(n)$ refers to the transmission window of the i-th ONU ($i=1,2,3$) on the n-th cycle time ($n=0,1,\ldots$).

In the first cycle time (observation cycle) the third ONU collects traffic from its user, four packets in this example. At the end of its transmission window (end of $V_3(1)$), this ONU sends a Report message to the OLT requesting a transmission window $V_3(2)$ of enough size to allocate such four packets in the next transmission window. In the next cycle time, the ONU receives a Grant message from the OLT and proceeds to transmit its four packets, under gated-service discipline. It is also worth noticing that the transmission window of the third ONU comprises a guard time (T_g in the figure) plus the transmission time of such four packets. In other words,

$$V_3(2)=T_g+\sum_{j=1}^{4}X_j \tag{1}$$

where the X_j values refer to the service time of the j-th packet, $j=1,2,3,4$ in this case.

The n-th cycle time, as observed by the third ONU, comprises the sum of transmission windows allocated to each ONU:

$$T_3(n)=\sum_{i=1}^{N}V_i(n) \tag{2}$$

Clearly, the transmission window for a particular ONU $V_i(n)$ depends on the size of its previous observation cycle time $T_i(n-1)$, i.e. the larger the size of $T_i(n-1)$ the more packets collected for the next transmission window. As noted from Fig. 1(b), a packet chosen at random (for instance packet number 4) must wait until the end of its current observation cycle time, then wait for the transmission window of the other ONUs ($V_1(2)$ and $V_2(2)$ in the figure), and finally wait for the guard time T_g and the other packets in the queue of its ONU (this is packets 1, 2 and 3). Next section reviews the steady-state values of V_i and T_i under Poisson traffic.

2.2. Analytical review under Poisson traffic

Consider a PON with N ONUs, each one offering Poisson traffic in the upstream direction with load ρ_i, $i=1,2,\ldots,N$, i.e. total offered load ρ, where

$$\rho=\sum_{i=1}^{N}\rho_i<1$$

Let T_g refer to the guard time between consecutive transmission windows, and let X_j denote the service time for the j-th packet. In this scenario, the transmission window for a given ONU is obtained as

$$V_i(n)=T_g+\sum_{j=1}^{N_p(T_i(n-1))}X_j \tag{3}$$

which is the sum of the guard time plus the service times of the packets received during its previous observation cycle, denoted as $N_p(T_i(n-1))$. The number of packet arrivals $N_p(t)$ for the i-th ONU within an observation cycle of length t is assumed to follow a Poisson process with rate

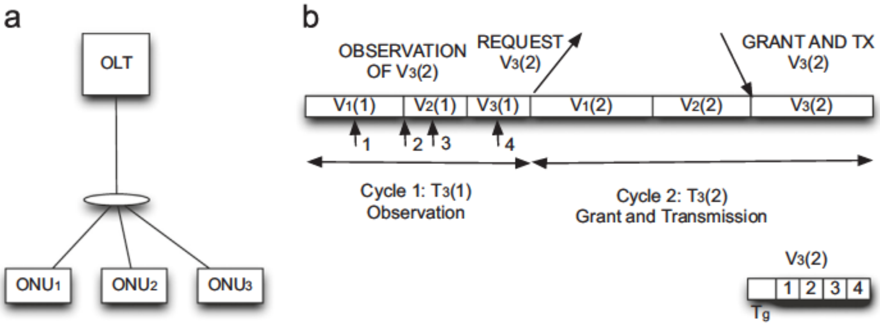

Fig. 1. Example of a PON with three ONUs and bandwidth sharing using IPACT. (a) PON topology with N=3 ONUs. (b) Example of TDM scheduling using IPACT.

λ_i packet/s:

$$P(N_p(T_i(n-1))=k)=\frac{(\lambda_i T_i(n-1))^k}{k!}e^{-\lambda_i T_i(n-1)}, \quad k\geq 0 \qquad (4)$$

The mean of such a Poisson process is known to be

$$E(N_p(T_i(n-1)))=\lambda_i E(T_i(n-1)) \qquad (5)$$

Hence, the average transmission window equals

$$E(V_i(n))=T_g+E(N_p)E(X)=T_g+\lambda_i E(T_i(n-1))E(X)$$
$$=T_g+\rho_i E(T_i(n-1)) \qquad (6)$$

where $E(X)$ refers to the average packet service time.

The variance follows

$$Var(V_i(n))=E(N_p)Var(X)+Var(N_p)(E(X))^2$$
$$=\lambda_i E(T_i(n-1))E(X^2) \qquad (7)$$

since $Var(N_p)=E(N_p)=\lambda_i E(T_i(n-1))$ for the Poisson process. Here, $E(X^2)$ refers to the second moment of random variable X.

Previous work has already shown that, in the steady-state, the average cycle time follows [4,5]:

$$E(T)=\sum_{i=1}^{N} E(V_i) \qquad (8)$$

since, in the steady state, $E(T_i(n-1))=E(T_i(n))$ and $E(V_i(n-1))=E(V_i(n))$, for $n=1,2,\ldots$.

Let us further consider that all ONUs offer the same traffic load to the PON, i.e. $\rho_i=\rho/N$, i=1,...,N. Solving Eqs. (6) and (8) brings

$$E(T)=\frac{NT_g}{1-\sum_i\rho_i}=\frac{NT_g}{1-\rho}=T_{ss} \qquad (9)$$

$$E(V_i)=T_g+\rho_i\frac{NT_g}{1-\rho}=\frac{T_g}{1-\rho}=V_{ss} \qquad (10)$$

Here, V_{ss} denotes the average transmission window in the steady-state for each ONU when all of them offer Poisson traffic with the same load ρ/N. Similarly, T_{ss} refers to the average cycle time in the steady-state as observed by the N-th ONU under Poisson traffic.

Numerical example: Consider two ONUs with the same load $\rho_i=0.1$, i=1,2 and guard time $T_g=5$ µs. Then

$$T_{ss}=\frac{NT_g}{1-\sum_i\rho_i}=\frac{2\times 5\ \mu s}{1-0.2}=12.5\ \mu s$$

and

$$V_{ss}=T_g+\rho_i T_{ss}=5\ \mu s+0.1\times 12.5\ \mu s=6.25\ \mu s$$

on average.

It is worth noticing that these values do not consider the average packet service time $E(X)$. In the case of an average packet size of 500 bytes, this value would be

$$E(X)=8\frac{500b}{10^9 b/s}=4\ \mu s$$

As noted, $V_{ss}-T_g$ is much smaller than $E(X)$. Essentially, this means that most of the time the ONUs request 0 packets and only sometimes, they do request one packet or more, yielding an average of $\rho_i T_{ss}=1.25$ µs of transmission time per cycle.

2.3. Delay analysis under Poisson traffic

Remark from [6] that the average queueing delay $E(W_q)$ experienced by a random packet in a PON arises as a modification of the M/G/1 queue with vacations formerly analysed in [7]:

$$E(W_q)=\frac{\lambda E(X^2)}{2(1-\rho)}+\frac{(3N-\rho)E(R)}{2(1-\rho)}+\frac{Var(R)}{2E(R)} \qquad (11)$$

where $E(X^2)$ refers to the second moment of the packet service time, and $E(R)$ and $Var(R)$ denote the average reservation time and its variance. In IPACT, the reservation time R is computed as the fixed transmission time of a 64-byte control packet containing the requested transmission window for the next time-slot. Hence, $E(R)=864b/(10^9 b/s)=1.512$ µs and $Var(R)=$ 0 a s n o t e d i n [6].

An alternative approach to obtain $E(W_q)$, which will be used in the rest of the paper, follows the next reasoning: consider that, during the observation cycle of the third ONU in the example of Fig. 1(b), only one packet arrives, i.e. N_p=1. Thanks to the properties of the Poisson process, such a packet arrives at any place within the observation cycle of the ONU with equal probability, i.e. it is uniformly distributed $U(0,T_{ss})$ in the steady-state. Hence, this packet must wait for the remaining time until the observation cycle is complete, plus two more transmission windows, plus guard time and its average service time $E(X)$. On average, this value is

$$E(W|N_p=1)=D_1(1)$$

$$=\frac{1}{2}T_{ss}+(N-1)V_{ss}+T_g+E(X)$$

where $D_i(N_p)$ refers to the average delay experienced by the i-th packet when $N_p \geq i$ packet arrivals have occurred during the observation cycle.

Now, consider the case that two packets arrive during the observation cycle of the third ONU, i.e. N_p=2. The first packet arrival time can be derived from the first order statistic in a sample of two uniformly distributed random variables within the time interval $(0, T_{ss})$. As shown in Fig. 2, the first packet must wait $\frac{3}{4}T_{ss}$ on average until the observation cycle concludes, whereas the second packet only needs to wait an average of $\frac{1}{4}T_{ss}$. On the contrary, the first packet is dispatched before the second packet, which has to wait an additional service time (the first packet's service time). Hence, the first packet experiences a total delay $D_1(2)$ of

$$D_1(2)=\frac{3}{4}T_{ss}+(N-1)V_{ss}+T_g+E(X)$$

whereas the second one experiences the following delay:

$$D_2(2)=\frac{1}{4}T_{ss}+(N-1)V_{ss}+T_g+2E(X)$$

The mean value for these two packets is

$$E(W|N_p=2)=\frac{1}{2}\sum_{i=1}^{2}D_i(2)=\frac{1}{2}T_{ss}+(N-1)V_{ss}+T_g+\frac{3}{2}E(X) \tag{12}$$

Following the same reasoning for three packet arrivals (i.e., N_p=3), we obtain

$$D_1(3)=\frac{5}{6}T_{ss}+(N-1)V_{ss}+T_g+E(X)$$

$$D_2(3)=\frac{3}{6}T_{ss}+(N-1)V_{ss}+T_g+2E(X)$$

$$D_3(3)=\frac{1}{6}T_{ss}+(N-1)V_{ss}+T_g+3E(X)$$

and the average is

$$E(W|N_p=3)=\frac{1}{3}\sum_{i=1}^{3}D_i(3)=\frac{1}{2}T_{ss}+(N-1)V_{ss}+T_g+2E(X) \tag{13}$$

In the generic case of $N_p=k$ packet arrivals, the average delay experienced by the j-th packet follows

$$D_j(k)=\frac{2k-2j+1}{2k}T_{ss}+(N-1)V_{ss}+T_g+jE(X)$$

and the weighted average delay for a random packet selected from those k packets is

$$\begin{aligned}E(W|N_p=k)&=\frac{1}{k}\sum_{j=1}^{k}D_j(k)\\&=\frac{1}{2}T_{ss}+(N-1)V_{ss}+T_g+\frac{k+1}{2}E(X)\\&=\frac{3N-2\rho}{2N}T_{ss}+\frac{k+1}{2}E(X)\end{aligned} \tag{14}$$

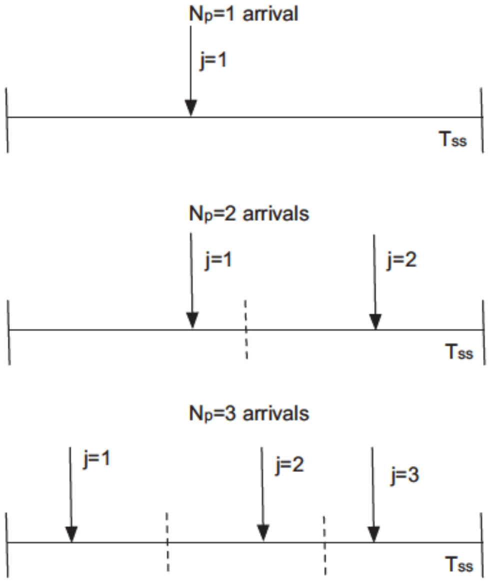

Fig. 2. Average arrival time of the j-th packet in a set of $N_p=k$ total packets, $k=1,2,3$.

Thus, the average total waiting time must weight each case with its probability

$$E(W)=\sum_{k=1}^{\infty}E(W|N_p=k)P(N_p=k) \tag{15}$$

where

$$P(N_p=k)=\frac{(\lambda_i T_{ss})^k}{k!}e^{-\lambda_i T_{ss}}$$

After some calculus, Eq. (15) becomes

$$E(W)=\frac{3N-\rho}{2N}T_{ss}+\frac{E(X)}{2}=\frac{3N-\rho}{2(1-\rho)}T_g+\frac{E(X)}{2} \tag{16}$$

Finally, it is worth noticing that the average queueing delay experienced by a random packet follows

$$E(W_q)=E(W)-E(X)=\frac{3N-\rho}{2(1-\rho)}T_g-\frac{E(X)}{2} \tag{17}$$

Numerical example: In the previous numerical example, we had two ONUs that offered Poisson traffic in the upstream channel with load: $\rho_i=0.1$, i=1,2. In this example, the average cycle time was computed as $E(T_{ss})=$ 12.5 µs and the average packet service time is $E(X)=4$ µs. The average delay experienced by a packet in a given ONU would then be

$E(W)=20.125$ µs

as it follows from Eq. (16).

3. Analysis of the effect of a peak of traffic

3.1. Transmission windows and cycle times

Next, we analyse the effect of a peak of traffic in the structure and properties of transmission window values V_i and cycle times T. Again, consider a PON with N ONUs offering Poisson traffic in the upstream direction with load ρ/N. Consider that the first ONU seldomly offers peaks of traffic in addition to its regular Poisson traffic. Such peaks comprise data bursts of length B μs every T_b units of time (for the sake of simplicity, we will consider[1] $T_b \to \infty$). Next, we study the impact of such a data burst on subsequent transmission windows. Essentially, the transmission window values V_i follow the next recurrence relationship

$$V_i(n) = T_g + \rho_i T_i(n-1), \quad i = 1, \ldots, N \tag{18}$$

where the $T_i(n-1)$ refers to the observation cycle time of the i-th ONU:

$$T_i(n-1) = \sum_{k=i+1}^{N} V_k(n-2) + \sum_{k=1}^{i} V_k(n-1) \tag{19}$$

Cycle 0: *Burst arrival.* Initially, all ONUs transmit their previously announced Poisson-shape received traffic. Recall from the previous section that, under Poisson traffic, the average transmission window offered by each ONUs is $V_{ss} = T_g/(1-\rho)$

$$V_1(0) = T_g + \frac{\rho}{N} T_{ss} = V_{ss}$$
$$V_2(0) = V_{ss}$$
$$\vdots \quad \vdots$$
$$V_N(0) = V_{ss}$$

The total cycle time then follows:

$$T_i(0) = T_{ss}, \quad i = 1, 2, \ldots, N \tag{20}$$

In addition, the first ONU has just received a peak of traffic, consequently it requests a grant for its transmission together with its regular Poisson traffic. Such a burst will be therefore transmitted in the next transmission window.

Cycle 1: *Burst transmission*. The first ONU transmits its Poisson traffic V_{ss} along with the data burst B. The other ONUs transmit their Poisson traffic announced in their previous observation cycle

$$V_1(1) = V_{ss} + B$$
$$V_2(1) = V_{ss}$$
$$\vdots \quad \vdots$$
$$V_N(1) = V_{ss}$$

after applying Eq. (18).

So the total cycle time is now

$$T_i(1) = \sum_{k=i+1}^{N} V_k(0) + \sum_{k=1}^{i} V_k(1) = NV_{ss} + B = T_{ss} + B, \quad i = 1, 2, \ldots, N \tag{21}$$

which shows an excess of B units of time with respect to $T_i(0)$ due to the first ONU's burst.

Cycle 2: *First cycle after burst transmission*. In this cycle, the first ONU transmits the Poisson traffic announced in its previous observation cycle. Obviously, such traffic volume is expected to be much higher than V_{ss} since the transmission of the data burst implies a longer period of data collection. This reasoning also applies to the other ONUs:

$$V_1(2) = T_g + \frac{\rho}{N}(NV_{ss} + B) = V_{ss} + \frac{\rho}{N} B$$
$$V_2(2) = V_{ss} + \frac{\rho}{N} B$$
$$\vdots \quad \vdots$$
$$V_N(2) = V_{ss} + \frac{\rho}{N} B$$

after applying Eq. (18).

As observed, the data burst transmitted in the first cycle time impacts the average transmission window of all ONUs equally. The total cycle time is therefore (Eq. (19))

$$\begin{aligned} T_i(2) &= \sum_{k=i+1}^{N} V_k(1) + \sum_{k=1}^{i} V_k(2) \\ &= (N-i)V_{ss} + i\left(V_{ss} + \frac{\rho}{N} B\right) \\ &= NV_{ss} + i\frac{\rho}{N} B = T_{ss} + i\frac{\rho}{N} B, \quad i = 1, 2, \ldots, N \end{aligned} \tag{22}$$

Interestingly, the average cycle time $T_i(2)$ has increased by a factor of $i(\rho/N)B$ with respect to $T_i(0)$, but is still much smaller than $T_i(1)$ which included the whole burst transmission B.

Cycle 3: *Second cycle after burst transmission*. Again, every ONU offers its traffic as was collected during its previous observation cycle. However, it is worth remarking that the transmission windows in the previous cycle are slightly larger than V_{ss} due to the impact of the previous data burst. After applying Eq. (18), this brings the following new transmission windows:

$$\begin{aligned} V_1(3) &= T_g + \frac{\rho}{N}\left((N-1)V_{ss} + \left(V_{ss} + \frac{\rho}{N} B\right)\right) \\ &= V_{ss} + \left(\frac{\rho}{N}\right)^2 B \\ V_2(3) &= T_g + \frac{\rho}{N}\left((N-2)V_{ss} + 2\left(V_{ss} + \frac{\rho}{N} B\right)\right) \\ &= V_{ss} + 2\left(\frac{\rho}{N}\right)^2 B \\ &\vdots \quad \vdots \\ V_N(3) &= T_g + \frac{\rho}{N}\left((N-N)V_{ss} + N\left(V_{ss} + \frac{\rho}{N} B\right)\right) \\ &= V_{ss} + N\left(\frac{\rho}{N}\right)^2 B \end{aligned} \tag{23}$$

As noted, the transmission windows experience a slight increase from one ONU to the next, with the last one, the N-th ONU, being the one with the largest transmission window. The reason for this is that the last ONU accumulates more Poisson traffic than any other, since its observation cycle time is larger than the others. In particular, it accumulates traffic for N times $V_{ss} + (\rho/N)B$. The new total cycle time, as observed by the i-th ONU, is (using Eq. (19))

$$\begin{aligned} T_i(3) &= \sum_{k=i+1}^{N} V_i(2) + \sum_{k=1}^{i} V_i(3) \\ &= (N-i)\left(V_{ss} + \frac{\rho}{N} B\right) + \sum_{k=1}^{i} \left(V_{ss} + k\left(\frac{\rho}{N}\right)^2 B\right) \\ &= (N-i)\left(V_{ss} + \frac{\rho}{N} B\right) + iV_{ss} + \frac{i(i+1)}{2}\left(\frac{\rho}{N}\right)^2 B \\ &= T_{ss} + (N-i)\frac{\rho}{N} B + \frac{i(i+1)}{2}\left(\frac{\rho}{N}\right)^2 B, \quad i = 1, 2, \ldots, N \end{aligned} \tag{24}$$

[1] Notice that, if a new burst arrives after the effect of the previous burst has vanished, we can consider that this analysis is still valid. In other case, the effects of one burst will overlap with the next one, which will not be analysed in this paper and it is left for future work.

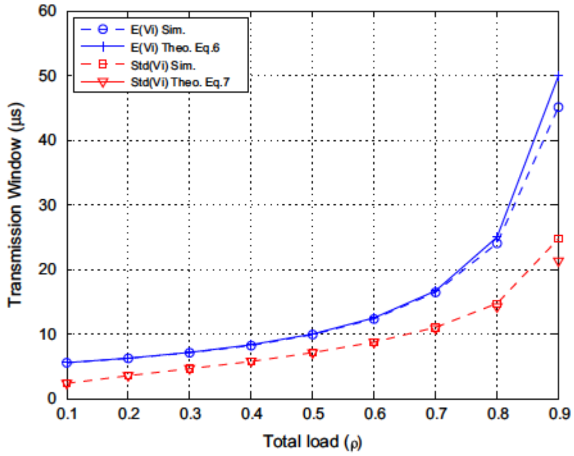

Fig. 3. Transmission window in the steady-state: expectation and standard deviation.

As shown, the impact of the data burst is much smaller on $T(3)$ than on $T(2)$ since it has a factor of ρ^2. This suggests that the impact of the data burst vanishes over time, which makes sense.

Subsequent cycle times: For subsequent cycle times, the transmission windows and cycle times can be derived from Eqs. (18) and (19).

3.2. Delay analysis under bursty traffic

This section aims at re-calculating the delay experienced by the packets in an ONU under bursty conditions. Following the reasoning of Section 2.3, the average delay observed by a random packet must take into account every possible number of packet arrivals N_p in its previous observation cycle (see Eq. (15)

$$E(W) = \sum_{k=1}^{\infty} E(W|N_p = k)P(N_p = k)$$

where each value in this equation varies with the transmission windows and cycle times computed before. Let $W_i(n)$ refer to the delay observed by the packets of the i-th ONU on the n-th cycle. Then, the average delay for packets of the i-th ONU when the size of the burst is $N_p = k$ can be obtained as

$$E(W_i(n)|N_p = k) = \frac{1}{2}T_i(n-1) + \left(\sum_{j=i+1}^{N} V_j(n-1) + \sum_{j=1}^{i-1} V_j(n)\right) + T_g + \frac{k+1}{2}E(X) \qquad (25)$$

For the sake of simplicity, next sections study the average delay for the N-th ONU during all the phases of burst arrival, transmission and subsequent cycles, although the same reasoning can be applied to the other ONUs.

Cycle 0: Burst arrival. The zero-th cycle is a steady-state cycle, thus following the same equations derived in Section 2.3:

$$E(W_N(0)|N_p = k) = \frac{1}{2}T_{ss} + (N-1)V_{ss} + T_g + \frac{k+1}{2}E(X) = \frac{3N-\rho}{2N}T_{ss} + \frac{k+1}{2}E(X) \qquad (26)$$

Cycle 1: Burst transmission. During the burst transmission cycle, the packets to be transmitted by the N-th ONU experience the following delay:

$$E(W_N(1)|N_p = k) = \frac{1}{2}T_{ss} + (N-1)V_{ss} + B + T_g + \frac{k+1}{2}E(X) = \frac{3N-\rho}{2N}T_{ss} + B + \frac{k+1}{2}E(X) \qquad (27)$$

So the packets transmitted in this cycle experience an extra delay of B units of time.

Cycle 2: First cycle after burst transmission. Packets to be transmitted at cycle 2 will observe the following delay:

$$\begin{aligned} E(W_N(2)|N_p = k) &= \frac{1}{2}T_N(1) + \sum_{i=1}^{N-1} V_i(2) + T_g + \frac{k+1}{2}E(X) \\ &= \frac{1}{2}(T_{ss} + \rho B) + (N-1)\left(V_{ss} + \frac{\rho}{N}B\right) \\ &\quad + T_g + \frac{k+1}{2}E(X) \\ &= \frac{3N-\rho}{2N}T_{ss} + \frac{3N-2}{2N}\rho B + \frac{k+1}{2}E(X) \end{aligned}$$

where the delay has been reduced with respect to the previous cycle by a factor of ρ, as expected, but still is much larger than $E(W_N(0)|N_p = k)$.

Subsequent cycle times: Finally, in subsequent cycle times, the recursive equation (25) needs to be applied to each particular case. The result observed is that packet delay after a number of subsequent cycle times n approaches the steady state of Eq. (26).

These equations are validated with simulation in the next section.

4. Validation via simulation

The following set of experiments aim at validating the theoretical results obtained throughout the paper via simulation. The discrete event-driven simulator was implemented in Matlab,[2] which allows to build an EPON with one OLT, several ONUs as well as the links connecting both ends. Unless otherwise stated, the simulations have been carried out with the following parameters:

- N — number of ONUs in the PON, default N=32.
- T_g — guard time value, default $T_g = 5$ μs.
- $E(X)$ — average packet service time, default $E(X) = 5$ μs. This is the transmission delay for a 624.22 byte-packet[3] over a 1 Gb/s link.
- B — burst transmission time, default 360 μs. This is the transmission time of a bunch of 30 packets of size 1500 bytes.

4.1. Transmission window in the steady state

Fig. 3 shows the steady-state transmission window values V_{ss} under Poisson traffic. As shown, the theoretical values for the average and standard deviation (Eq. (6) and

[2] http://www.mathworks.es/products/matlab/

[3] This is the average packet size obtained from the measurements in [21,22].

the square root of Eq. (7) respectively) perfectly match the simulation results at medium and low loads, and slightly deviate at high loads. This result is consistent with previous works from [4,5].

4.2. *Average queueing delay $E(W_q)$ under Poisson traffic*

Fig. 4 shows the average queueing delay experienced by packets of a given ONU under Poisson traffic only. The results show both the delay obtained via simulation along with the theoretical formula presented in [6] and our method presented in Section 2.3 (Eq. (17)). As shown, both theoretical methods overlap with the simulation results, thus validating both equations and methodologies.

4.3. *Effect of a peak of burst*

Fig. 5(a), (b) shows the values of the transmission windows of each ONU $V_i(n)$ derived in Section 3.1 at different load levels. The $V_i(n)$ values are depicted in a semilogy axis for a better visualisation. The *x*-axis represents the index $N \cdot n+i$, this means that the $V_i(n)$ values for the *i*-th ONU are depicted in positions $i+32 \cdot n$ (i.e., 1, 33, 65, 97…for the first ONU; 2, 34, 66, 98…for the second ONU and so on). As shown, both theoretical and simulated values perfectly match, thus validating the results obtained in Section 3.1.

The figures show that at low loads, the transmission windows quickly recover to the steady state value V_{ss} or something very close to it. Essentially, after the burst transmission (this is $V_1(1)=V_{ss}+B$ on the first cycle), all ONUs experience the same transmission window in cycle two: $V_i(2)=V_{ss}+(\rho/N)B$. The third and fourth cycles show some excess with respect to V_{ss} only at high loads, since at low loads the effect is very small. After the fourth cycle, the peak effects reduce dramatically showing a very limited impact on the values of the transmission windows $V_i(n)$.

As noted in the previous section, the size of a given transmission window depends on the length of its observation cycle $T_i(n-1)$ and its load ρ_i. Hence, when the burst transmission lies in the observation cycle of an ONU, the transmission window is expected to be large since more traffic has been accumulated by the ONU. In subsequent cycles, the observation periods decrease, hence the effects of the data burst vanish over time. The speed at which the cycle times approach the steady state value T_{ss} depends on the burst size B and the current Poisson network load ρ, a s demonstrated in Section 3.1.

The next section studies the impact of a peak of traffic in terms of average delay experienced by the different ONUs.

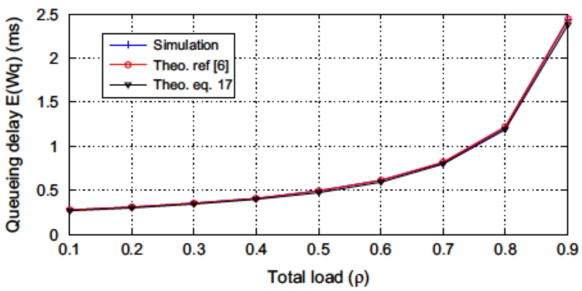

Fig. 4. Average queueing delay $E(W_q)$ under Poisson traffic.

4.4. *Average packet delay under bursty traffic*

Fig. 6(a), (b) shows the average delay experienced by the packets of some ONUs during the different stages of a data burst (arrival, transmission and after transmission), at different network loads. As observed, the first ONU (ONU=1 in the figure) experiences a high delay peak during the burst transmission (cycle number one), while the others only experience a moderate delay increase with respect to the average delay in the steady-state.

In the second cycle, all ONUs have a very similar average delay, which is expected since they have a similar observation cycle. However, the last ONU always experiences a slightly larger delay than the others in the second cycle. This behaviour remains for the third cycle, but on the fourth cycle, it is the first ONU which experiences slightly more delay than the others. Finally, in subsequent cycles, the average delay decreases approaching the average delay value in the steady-state.

4.5. *A study of the vanishing time of a burst*

This experiment further investigates the vanishing time of a data burst for several burst sizes and at different load conditions. We define the vanishing time T_{vanish} as the amount of time required to achieve a nearly-stable transmission window (i.e. $V_i \leq 1.1V_{ss}$) after the arrival and transmission of a data burst. Clearly, T_{vanish} defines a metric that features the time required to have almost no residual effect of the burst transmission in the PON.

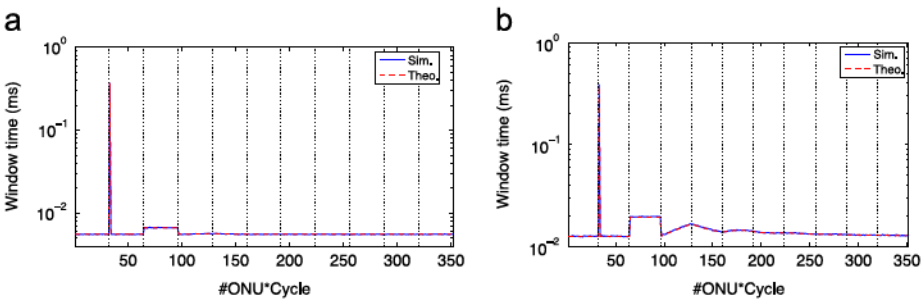

Fig. 5. Average transmission window $V_i(n)$ in different cycle times. (a) $\rho=0.1$. (b) $\rho=0.6$.

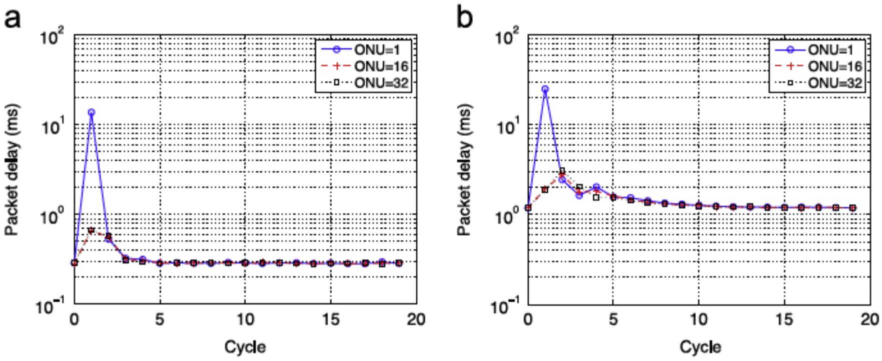

Fig. 6. Average delay experienced by random packets during the burst arrival and subsequent cycles. (a) $\rho = 0.1$. (b) $\rho = 0.6$.

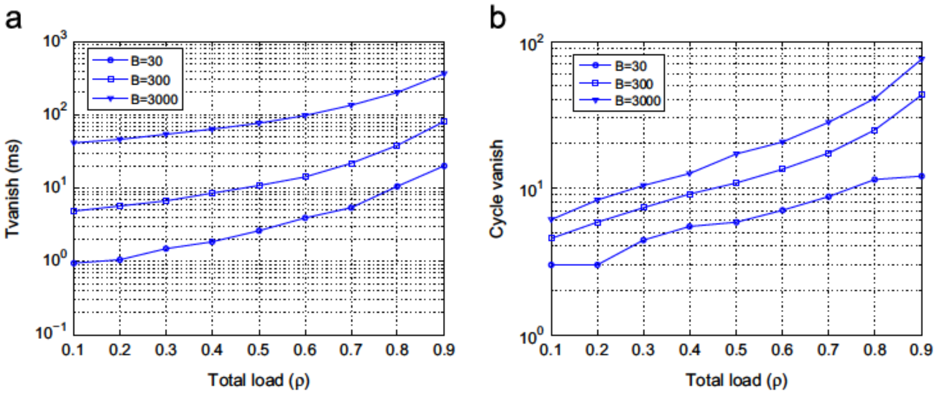

Fig. 7. Evolution of T_{vanish} for several burst sizes at different loads. (a) Packet delay (ms). (b) Cycle number.

Fig. 7(a), (b) shows some numbers of the T_{vanish} metric obtained via simulation under different network conditions and burst sizes ($B=\{30,300,3000\}$ packets of 1500 bytes). The former figure shows the average amount of time required to achieve nearly steady-state conditions ($V_i \le 1.1V_{ss}$). The second figure shows the cycle at which this condition occurs.

As shown, at low loads ($\rho \le 0.3$), T_{vanish} remains low and stable in milliseconds (Fig. 7(a)). Furthermore, at load $\rho = 0.3$, Fig. 7(b) shows that about 3, 6 and 10 cycles are required to achieve the vanishing condition of $1.1V_{ss}$ for $B=30$, 300 and 3000 respectively.

However, at medium and high loads, the value of T_{vanish} increases very quickly. This proves the fact that the vanishing time depends not only on the burst size itself, but also on the total load of the PON.

5. Summary and discussion

This paper has studied the effect of data bursts in the upstream channel of Ethernet Passive Optical Networks employing IPACT under the gated-service discipline. Essentially, a mathematical model is provided to derive the average transmission windows of every ONU at different situations under the presence of data bursts: burst arrival, transmission and after transmission. The effect of such a data burst has been studied from both the perspective of the average cycle time observed by the OLT in the PON, the transmission window dynamics, and the actual delay experienced by packets of other ONUs waiting for a granted transmission window.

From mathematical analysis and simulation, we observe that the effects of a data burst propagate to subsequent cycles, thus affecting other users and their delay experienced. The time until the negative effects of such a data burst vanish over time varies depending on both the actual burst size and network load, going from a few milliseconds (small bursts) to possibly some tens and even hundreds of milliseconds, especially at high loads.

Future work will use the methodology presented in this paper through Section 3 to study other Dynamic Bandwidth Allocation disciplines, for instance, the limited service discipline.

Acknowledgements

The authors would like to thank the reviewers for their valuable comments through the reviewing process of this paper. The authors would also like to acknowledge the Spanish-funded CRAMnet (Grant no. TEC2012-38362-C03-01) and the Madrid Community MEDIANET (S2009-TIC1468) projects for their support to this work.

References

[1] G. Kramer, Ethernet Passive Optical Networks, McGraw-Hill, (New York, USA), 2005. ISBN-13: 978-0071445627.

[2] G. Kramer, B. Mukherjee, Pesavento, IPACT: a dynamic protocol for an Ethernet PON (EPON), IEEE Commun. Mag. 40 (2) (2002) 74–80.[3] M. McGarry, M. Maier, M. Reisslein, Ethernet PONs: a survey of dynamic bandwidth allocation (DBA) algorithms, IEEE Commun. Mag. 42 (8) (2004) 8–15.

[4] B. Lannoo, L. Verslegers, D. Colle, M. Pickavet, M. Gagnaire, P. Demeester, Analytical model for the IPACT dynamic bandwidth allocation algorithm for EPONs, OSA J. Opt. Netw. 6 (6) (2007) 677–688.

[5] F. Aurzada, M. Scheutzow, M. Herzog, M. Maier, M. Reisslein, Delay analysis of Ethernet Passive Optical Networks with gated service, OSA J. Opt. Netw. 7 (1) (2008) 25–41.

[6] S. Bharati, P. Saengudomlert, Analysis of mean packet delay for dynamic bandwidth allocation algorithms in EPONs, IEEE/OSA J. Lightwave Technol. 28 (23) (2010) 3454–3462.

[7] D. Bertsekas, R. Gallager, Data Networks, 2nd ed. Prentice Hall, (New Jersey, USA), 1992. ISBN 0-13-200916-1.

[8] C.-C. Sue, H.-W. Cheng, A fitting report position scheme for the gated IPACT dynamic bandwidth algorithm in EPONs, IEEE/ACM Trans. Netw. 18 (2) (2010) 624–637.

[9] P. Garfias, L. Gutiérrez, S. Sallent, Enhanced DBA to provide QoS to coexistent EPON and 10G-EPON networks, IEEE J. Opt. Commun. Netw. 4 (12) (2012) 978–988.

[10] T. Berisa, Z. Ilic, A. Bazant, Absolute delay variation guarantees in passive optical networks, IEEE/OSA J. Lightwave Technol. 29 (9) (2011) 1383–1393.

[11] I. Seoane, J.A. Hernández, R. Romeral, D. Larrabeiti, Analysis and simulation of a delay-based service differentiation algorithm for IPACT-based PONs, Photonic Netw. Commun. 24 (3) (2012) 228–236.

[12] F. Aurzada, M. Scheutzow, M. Reisslein, N. Ghazisaidi, M. Maier, Capacity and delay analysis of next-generation passive optical networks (NG-PONs), IEEE Trans. Commun. 59 (5) (2011) 1378–1388.

[13] M. Kiaei, K. Fouli, M. Scheutzow, M. Maier, M. Reisslein, C. Assi, Delay analysis for ethernet long-reach passive optical networks, in: Proceedings of IEEE International Conference on Communications (ICC), 2012, pp. 3099–3104.

[14] A. Dixit, B. Lannoo, G. Das, D. Colle, M. Pickavet, P. Demeester, Flexibility evaluation of hybrid WDM/TDM PONs, in: 2011 IEEE 5th International Conference on Advanced Networks and Telecommunication Systems (ANTS), IEEE, 2011, pp. 1-6 December 18-21, 2011. Bengaluru, India. doi: 10.1109/ANTS.2011.6163650.

[15] M. Bokhari, P. Saengudomlert, Analysis of mean packet delay for upstream transmissions in passive optical networks with sleep mode, Opt. Switch. Netw. 10 (3) (2013) 195–210.

[16] J.A. Hernández, I. Seoane, R. Romeral, D. Larrabeiti, A note on the potential energy savings by extending the average cycle times in Passive Optical Networks, in: Proceedings of European Conference on Networks and Optical Communications (NOC), 2012, pp. 1–4.

[17] S.H. Newaz, A. Cuevas, G.M. Lee, N. Crespi, J.K. Choi, Evaluating energy efficiency of ONUs having multiple power levels in TDM-PONs, IEEE Commun. Lett. 17 (6) (2013) 1248–1251. doi: 10.1109/LCOMM.2013.043013.122648.

[18] I. Cerutti, K. Abdallah, P.G. Raponi, P. Castoldi, Modeling and optimizing the delay-energy tradeoff in TDM systems with sleep mode, in: Proceedings of International Conference on Communications, 2012, pp. 236–241.

[19] P. Ameigeiras, J. Ramos-Muñoz, J. Navarro-Ortiz, J.M. Lopez-Soler, Analysis and modelling of youtube traffic, Trans. Emerg. Telecommun. Technol. 23 (4) (2012) 360–377.

[20] A. de la Oliva, T.R. Vargas Hernández, J.C. Guerri, J.A. Hernández, P. Reviriego, Analysis of energy efficient ethernet on video streaming servers, Comput. Netw. (3) (2013) 599–608.

[21] C.G. Park, D.H. Han, K.W. Rim, Packet delay analysis of symmetric gated polling system for DBA scheme in a PON, Telecommun. Syst. 30 (1–3) (2005) 13–34.

[22] G.e.a. Kramer, On supporting differential classes of service in Ethernet Passive Optical Networks, OSA J. Opt. Netw. 1 (8–9) (2002) 280–298.